Modelling of Pneumatic Air Muscles for Direct Rotary Actuation of Hand Rehabilitation Glove

Boran Wang, Kean C. Aw, Morteza Biglari-Abhari, and Andrew McDaid

University of Auckland,
Faculty of Engineering, New Zealand
{bwan055,k.aw,m.abhari,andrew.mcdaid}@aucklanduni.ac.nz

Abstract. Pneumatic muscle actuator (PMA) has the virtue of lightness, high power to weight ratio, small size, simple customization, easy fabrication, no stiction, inherent compliant behaviour and low cost. Hence, it has great potential as an actuator for hand rehabilitation device. Its stretchability and soft nature makes it easy to be mounted on curved surface and bend around corner. It is also able to produce very high forces over reasonable contraction. Here, we will present the use of PMA as a direct rotary actuator for hand rehabilitation glove. A model will be developed and verified experimentally for the PMA used in this configuration.

Keywords: pneumatic air muscle, hand rehabilitation, rotary actuator.

1 Introduction

Stroke is a common condition, which contributes substantially to disability around the world. Although the death rate per capita in New Zealand has declined steadily over the last 20 years, the total number of deaths from stroke increases as a result of increase in the total population [1]. Many reports suggest that the most effective way of relearning motor function is through carefully directed, well-focused, intensive and repetitive practice of the impaired hand [2-4]. With an aging population and limited hospital resources, the demand for robot-aided training program to replace the conventional labour-intensive rehabilitation technique increases. The idea of developing a robotic exoskeleton for hand rehabilitation has been widely recognized only over the last decade [5]. Existing grounded exoskeletons are sophisticated enough to facilitate a systematic post-stroke hand training program but they cannot be adapted to an easy-manipulated home-based training protocol because of their large volume, heavy weight or high cost [6-8]. They need to be robust but mechanical lightweight, resourceful control technology and compact power unit [9-11]. Without considering the human hand anatomy in depth, each single joint is actuated by one set of actuators, resulting in a device with high mechanical complexity. More recent designs take the natural coupling of distal interphalangeal (DIP) and proximal interphalangeal (PIP)

M. Beetz et al. (Eds.): ICSR 2014, LNAI 8755, pp. 360–369, 2014.

joints into consideration by activating PIP and metacarpal-phalangeal (MCP) joints only, hence reducing the weight and volume further. However, most of them are still using rigid components to build exoskeleton, which would possibly arouse heightened discomfort during training. This project aims to design a jointless rehabilitation glove completely using flexible actuators by treating user's hand itself as a skeletal structure. Targeted users are those with hypertonia and require long term self-motivated post stroke recovery training. As a proof of concept, this paper mainly focuses on the validation of using pneumatic air muscle (PMA) to generate rotary movements of user's affected unhealthy hand..

2 Construction of PMA

There are two primary components in fabricating an air muscle: a soft stretchable inner rubber tube and braided polyester mesh sleeve (Fig.1 (a)). The mesh sleeve is made in a crescent shape; as such it could bend around finger joint with its far side to human hand longer than the proximal side (Fig.1 (b)).

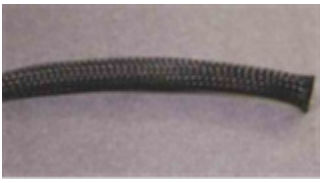

(a)

(b)

Fig. 1. Pictures of PMA (a) external braid with singed end, (b) fully constructed

3 Preliminary Testing

The optimum result in preliminary test have shown that a PMA of 60 mm long, 8 mm inner diameter and 25 mm outer diameter at 3.5 bar could lift up a test plastic finger with 50 g load by ~50° from a vertical flexed position.

4 Characterisation and Modelling in Bending Moment Application

Empirical modelling, which focuses on the concepts of observation and data fitting from real experiments was used to characterize the behaviour of the PMA. A mathematical model was established and validated both deductively based on its geometric structure and inductively through empirical findings. A finite element analysis will be performed in the future to optimize the dimension of PMA, but it is not within the scope of this paper.

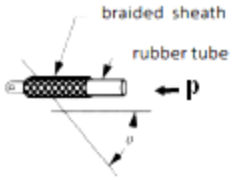

Fig. 2. Braid angle of PMA

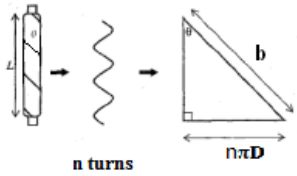

Fig. 3. Geometry of PMA

There are mainly five factors that determine the behaviour of PMA: pressure, sleeve diameter, sleeve length, diameter of inner tube and braided angle (Fig. 2 and 3). The air pressure can determine the stiffness of PMA, while greater sheath diameter increases the force. Longer PMA yields larger working range of movement but were unable to lift heavy load at the finger. The experiment set-up in Fig.4 (a) shows the PMA was attached to artificial hand and regulated by solenoid valves. Fig.4 (b) shows a picture of the set-up. Experimentally, a finger with a PMA of 40 mm length and 10 mm diameter with a perpendicular distance of 1 cm (d_3) from the joint could sustain a weight of 80 g with a pressure of 3.5 bar. The change in stiffness due to the pressure and shape provides an upward force to lift the finger.

4.1 Force and Contraction

For a given amount of air flow (p), work input to inflate the PMA and work output to generate deformation is $\boldsymbol{dW_{in} = p \times dV}$, and the work output produced in contracting the PMA is $\boldsymbol{dW_{out} = -F \times dx}$, where x is contracted length of PMA; F denotes the surface tension in PMA; V is the PMA volume. By ignoring energy loss due to frictions, the input energy should be equal to output energy, i.e. $\boldsymbol{dW_{in} = dW_{out}}$, which then gives

$$p \times dV = -F \times dx \tag{1}$$

According to Fig. 2 and 3, the geometric relationship of L (PMA length), D (diameter of PMA at specific pressure), b (PMA's braid length) and n (the number of turns of the braid) can be derived as:

$$D^2 = \frac{b^2 - L^2}{(n\pi)^2} \tag{2}$$

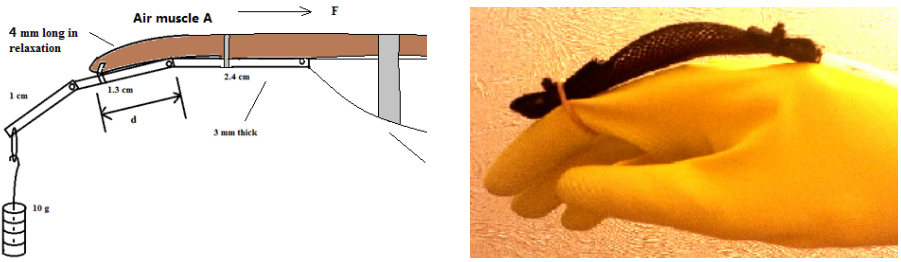

(a) (b)

Fig. 4. PMA attached to artificial finger (a) a schematic of experiment setup, (b) a picture of the experiment set-up

By assuming the PMA as a perfect cylinder, its volume can be expressed as:

$$V = \frac{\pi(b^2 - L^2)}{4(n\pi)^2} L = \frac{b^2 L - L^3}{4\pi n^2} \tag{3}$$

In a bending moment application, the shape of air muscle must not be a perfect cylinder. Thus the force tangential to bending surface is derived as

$$F = -p\frac{dV}{dL} = -p\frac{(b^2 - 3L^2)}{4\pi n^2} \tag{4}$$

The tension force produced by PMA can be expressed as

$$F = -p\frac{(b^2 - 3\left(L(1-\varepsilon)\right)^2)}{4\pi n^2} \tag{5}$$

where L_m is the maximum length of PMA; ε is percentage of change in length due to contraction. Equation (5) can be rearranged as a polynomial expression, i.e.

$$F = c_0\frac{pb^2}{4\pi n^2} + \frac{3pL}{4\pi n^2}(c_1 + c_2\varepsilon + c_3\varepsilon^2) \tag{6}$$

To validate the hypothesis, a series of experiments were run with different *p, b, L, n* and ε. The coefficients in Equation (6) were found with Matlab® data fitting tool. Experiments were carried out with very limited amount of pre-loading (< 5%) of the PMA to reduce discomfort to the wearer and Fig. 5 shows the result. Coefficients are computed with a 95% confidence interval. With the absolute pressure varying from 1 to 3.5 bar, the coefficients remained reasonably consistent. The final coefficients with a goodness of fit (R^2) ranging from 0.8974 to 0.9662 are:-

$$c_0 = 0.00625, c_1 = -0.0130, c_2 = 0.0321, c_3 = -0.140$$

$$F = 0.00625\frac{pb^2}{4\pi n^2} + \frac{3pL}{4\pi n^2}(-0.0130 + 0.0321\varepsilon - 0.140\varepsilon^2) \tag{7}$$

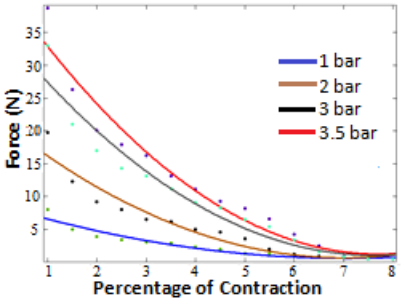

Fig. 5. Fitting of force against percentage contraction in PMA

As shown in Fig. 6 (a) the tension force along the PMA can be separated into two components: normal to the interacting surface $(\boldsymbol{F \times sin\alpha \times d_1})$ and parallel to the surface $(\boldsymbol{F \times cos\alpha \times d_2})$. Both components generate clockwise moment. However, when PMA is straightened, the bending moment decreases very quickly due to a drop in tension force. When α is ~ 50°, the resultant bending moment is ~ 0 and is unable to lift the finger up to a horizontal position. To increase bending moment, the distance between parallel component $(\boldsymbol{F \times cos\alpha \times d_2})$ and pivot (d_2) was raised up by increasing d_3 as in Fig. 6 (b). The simulated active torque against bending angle (α) with increasing d_3 from 0 to 3 cm with 1 cm increment is shown in Fig.8. A greater perpendicular distance would generate more torque, but could also result in a higher profile. Typical value for hypertonia/spasticity is ~0.4 Nm to rotate the finger joint by 90° [12] and can be achieved with d_3 = 3 cm (Fig. 7). It is able to fully extend a finger with a load of 50 g to a horizontal position.

4.2 Influence of Pressure

The contraction force generated by PMA is positively proportional to the internal air pressure *(p)* but there will be a limit for *p* in a real application as the PMA will burst. Here, the use 3.5 bar with the inner tube diameter of 6 mm is found to be safe.

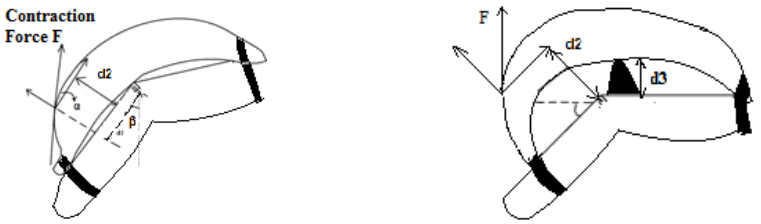

(a) (b)

Fig. 6. A schematic diagram (a) for force analysis, (b) showing the increase in active torque by increasing d_3

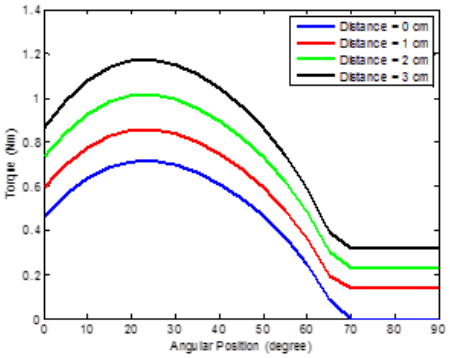

Fig. 7. Simulated result when d_3 has been changed

4.3 Influence of Braid Angle

Dynamic Analysis

To generate a model between braid angle and force, the relation between PMA's volume and braid angle was developed by assuming the pressurized PMA as a perfectly symmetrical cylinder with zero wall thickness. By assuming θ is the PMA's braided angle, the PMA's volume can be expressed as

$$V = \frac{1}{4}\pi D^2 L = \frac{b^3}{4\pi n^2}\sin^2\theta\cos\theta = \frac{b^3}{4\pi n^2}(\cos\theta - \cos^3\theta) \tag{8}$$

To find the maximum angle, both sides of equation were differentiated.

$$\frac{dV}{d\theta} = \frac{b^3}{4\pi n^2} \times (-\sin\theta + 3\cos^2\theta \times \sin\theta) \tag{9}$$

Therefore the tension force could be expressed as follows.

$$F = -p\frac{dV}{dL} = -p\frac{dV/d\theta}{dL/d\theta} = \frac{pb^2(3\cos^2\theta - 1)}{4\pi n^2} \tag{10}$$

By solving the equation, the maximum amount of contraction occurs when $\boldsymbol{F = 0}$ when $\theta = 54.7°$.

Static Analysis

The force in the PMA is separated into normal and longitudinal components by ignoring frictions between braids and braid thickness.

(a) (b)

Fig. 8. Force analysis (a) in longitudinal direction, (b) in normal direction

In longitudinal direction, the contraction force and normal component of the tension force in the sleeve are balanced (Fig. 8 (a)). If the total number of threads is *t*, then

$$F + \frac{\pi D^2}{4}p = F_N = t \times f_N \tag{11}$$

In normal direction, force yielded by internal air pressure is balanced by the longitudinal component of tension force in sleeve (Fig. 8 (b)).

$$pDL = 2F_L = t \times f_L \tag{12}$$

Given $tan\theta = \mathrm{f_L}/\mathrm{f_n}$, an expression of tension force can be obtained as

$$F = \frac{\frac{PDL\times\cos\theta}{2} + \frac{\pi}{4}D^2P\sin\theta}{\sin\theta} = \frac{pb^2(3\cos^2\theta - 1)}{4\pi n^2} \tag{13}$$

Equations (13) and (10) are similar, which means both dynamic and static methods generate the same result. The expression of force in terms of braided angle indicates as braid angle θ increases, the tension force generated by PMA will decrease, and is consistent with the experimental result. To verify the model, experiments were carried out by making the number of turns (*n)* constant, but changing the diameter and length of air muscle, so that the braid angle can be obtained by rearranging Equation (2).

The simulated plot (Fig. 9) of volume vs. braided angle indicates volume of air muscle keeps increasing until it reaches 54° when it begins to drop again. In practice, the PMA can burst when it reaches the maximum volume at a braided angle of

approximately 50°. In Fig. 10, the experimental results match reasonably well with simulation plot. Systematic error between them could be due to internal frictions between rubber tubes and braid sheath, as well as different constraint conditions on producing the air muscle. The fluctuation in force response could be due to sharp angles in finger joints when the PMA was first actuated from its vertical flex position.

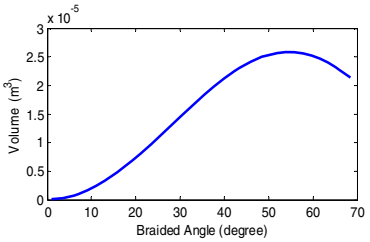

Fig. 9. Simulated result of volume vs. braided angle

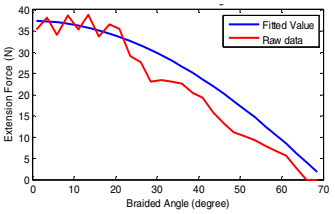

Fig. 10. Plot of force against braid angle

4.4 Influence of Braid Length

The experimental data matches well with the geometric model that there is a quadratic correlation between extension forces and braid length (Fig. 11). Mathematical modelling gives a goodness of fit (R^2) of 0.9606 to 0.9874. Experiments were carried out by setting pressure and braided angle constant, and measuring the forces generated by the PMA of different lengths. The coefficient (c_0) did not remain consistent as in Section 4.1 and this could be due to the random variation in the PMA. The final optimised PMA is 80 mm long and which is capable of lifting up a single finger digit from full flexion to a horizontal position.

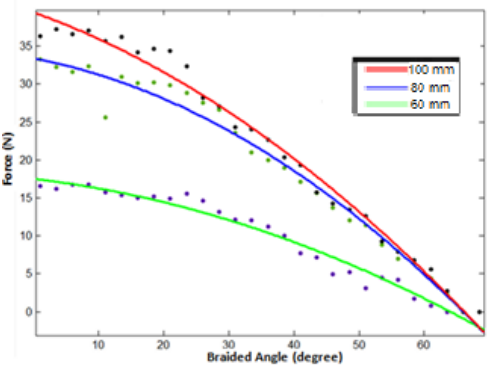

Fig. 11. Plot of contraction against sleeve length

Discussions and Future Work

The main limitation of a typical PMA is that it can only be actuated in a single direction. Since flexor hypertonia (the hand can only maintain a flexed position due to extensor weakness) is the most prevalent syndrome in stroke patients, the solution presented here could have a significant contribution to post-stroke hand rehabilitation. Even though the PMA requires an additional air compressor as its power source, the air pressure needed to actuate each finger was estimated to be 3.5 bar, which could be supplied by a compact, miniaturized air compressor.

(a) (b)

Fig. 12. Illustrations of (a) PMAs attached to testing rig, (b) a complete rehabilitation glove

As illustrated in Fig. 12. (a) and (b), the ultimate goal of this project is to develop and validate a multi-fingered model of a hand rehabilitation glove. Based on the model developed here, the dimension, material and shape of PMA can be optimized to minimize the weight of device and maximize the extension force. The proposed design has the potential to distinguish itself from other similar designs because of its highly complaint feature, low mechanical complexity and low profile.

Conclusions

This paper proposes a rotary movement of human finger joints for rehabilitation using flexible PMAs. The mathematical model was developed based on the dynamic and static analysis, verified and optimised through iterative tuning. Characterization of PMA considering the three most important factors; braided angle, pressure and braid length shows that a 80 mm long PMA, with one of its end fixed to the dorsal side of palm, is capable of fully rotating a finger joint with a pressure of 3.5 bar .

References

1. Mortality and Demographic Data (2009), http://www.health.govt.nz/publication/mortality-and-demographic-data-2006
2. Peter Langhorne, F.C.: Alex Pollock: Motor recovery after stroke: a systematic review. Lancet Neurol. 8, 741–754 (2009)
3. Krichevets, A.N., Sirotkina, E.B., Yevsevicheva, I.V., Zeldin, L.M.: Computer games as a means of movement rehabilitation. Disabil. Rehabil. 17(2), 100–105 (1995)

4. Biitefisch, C., Hummelheim, H., Denzler, P., Maurit, K.-H.: Repetitive training of isolated movements improves the outcome of motor rehabilitation of the centrally paretic hand. J. Neuro Sci. 130, 59–68 (1995)
5. Pilwon, H., Soo-jin, L., Kyehan, R., Jung, K.: Current Hand Exoskeleton Technologies for Rehabilitation and Assistive Engineering. Int. J. Precis. Eng. Man. 13(5), 807–824 (2012)
6. Dovat, L., Lambercy, O., Roger, G., Thomas, M., Ted, M., Teo Chee, L., Etienne, B.: HandCARE. IEEE Trans. Neural Syst. Rehabil. Eng. 16(6), 582–591 (2008)
7. Christopher, N.S., Rahsaan, J.H., Peter, S.L.: Development and pilot testing of HEXORR: Hand EXOskeleton Rehabilitation Robot. J. Neuroeng. Rehabil. 7(1), 1–16 (2010)
8. Satoshi Ueki, H.K., Satoshi, I., Yutaka, N., Motoyuki, A., Takaaki, A., Yasuhiko, I., Takeo, O., Tetsuya, M.: Development of a Hand-Assist Robot With Multi-Degrees-of-Freedom for Rehabilitation Therapy Satoshi. IEEE Intelligent Robots and Systems 2012 17(1), 136–146 (2012)
9. Devaraj, H.: Design and Development of a Portable Five-Fingered Hand Rehabilitation Exoskeleton, in Mechanicial Engineering Department, The University of Auckland I (2012)
10. John, B.M., Ralph, O.B., Dawn, B.M.: The SMART(R) Wrist-Hand Orthosis (WHO) for Quadriplegic Patients. J. Prosthet. Orthot. 5, 73–76 (1993)
11. Hommel, A., Wang, G.: Development and Control of a Hand Exoskeleton for Rehabilitation of Hand Injuries. In: IEEE Intelligent Robots and Systems 2005, pp. 3046–3051 (2005)
12. Popescu, D., Ivanescu, M., Popescu, D., Vladu, C., Vladu, I.: Force observer-based control for a rehabilitation hand exoskeleton system. In: 9th Asian Control Conference (2013)